4. Biophysics of the Cell Nucleus (1)

d. Cell mitosis

Lit.: - S. W. Grill et al, Nature, Vol 409, 2001
- S. W. Grill et al, PRL, 92, 2004
- S. W. Grill et al, Science, Vol 301, 2003

show figure 19-34

show figure 19-36

- Asymmetric cell divisions in C elegans embryos by spindle positioning:

  remove central spindle with an ultraviolet laser microbeam (show figure 1)

  ⇒ pulling forces exerted to the spindle act on the two spindle poles!

  ⇒ division of embryos generates a large anterior and a smaller posterior blastomer by a stronger net force acting on the posterior pole

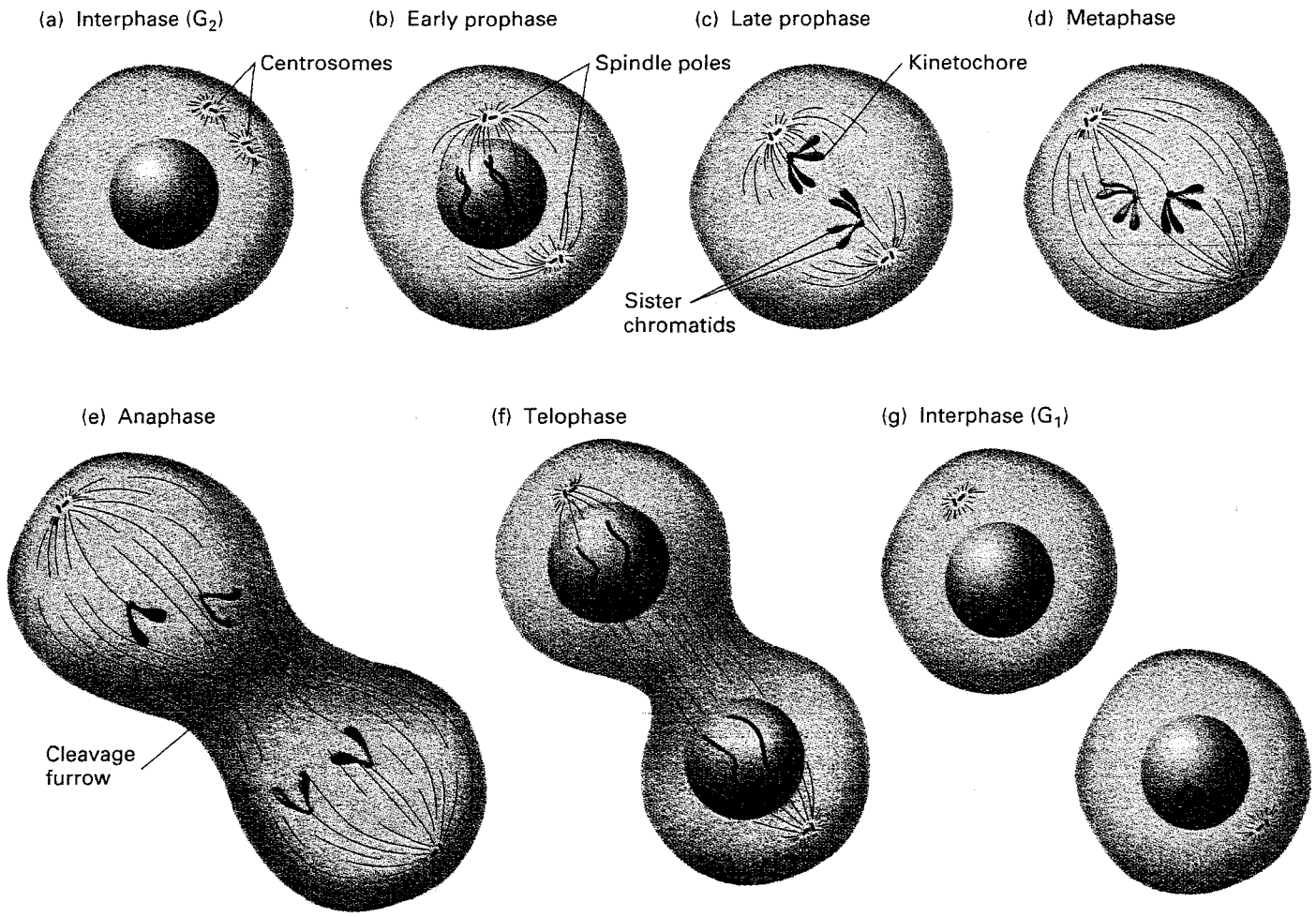

▲ **FIGURE 19-34 The stages of mitosis and cytokinesis in an animal cell.** (Morphological types of chromosomes are distinguished by color.) (a) *Interphase:* The G_2 stage of interphase immediately precedes the beginning of mitosis and follows chromosomal DNA replication during the S phase. The chromosomes, each containing a sister chromatid, are still dispersed and not visible as distinct structures. During interphase, the centrioles also are replicated, forming small daughter centrioles. (b) *Early prophase:* The centrosomes, each with a daughter centriole, begin moving toward opposite poles of the cell. The chromosomes can be seen as long threads, and the nuclear membrane begins to disaggregate into small vesicles. (c) *Middle and late prophase:* Chromosome condensation is completed; each visible chromosome structure is composed of two chromatids held together at their centromeres. The microtubular spindle fibers begin to radiate from the regions just adjacent to the centrosomes, which are moving closer to their poles. Some spindle fibers reach from pole to pole; most go to chromatids and attach at kinetochores. (d) *Metaphase:* The chromosomes move toward the equator of the cell, where they become aligned in the equatorial plane. The sister chromatids have not yet separated. This is the phase in which morphological studies of chromosomes are usually carried out. (e) *Anaphase:* The two sister chromatids separate into independent chromosomes. Each contains a centromere that is linked by a spindle fiber to one pole, to which it moves. Simultaneously, the cell elongates, as do the pole-to-pole spindles. Cytokinesis begins as the cleavage furrow starts to form. (f) *Telophase:* New nuclear membranes form around the daughter nuclei; the chromosomes uncoil and become less distinct; and the nucleolus becomes visible again. Cytokinesis is nearly complete, and the spindle disappears as the microtubules and other fibers depolymerize. Throughout mitosis the "daughter" centriole at each pole grows, so that by telophase each of the emerging daughter cells has two full-length centrioles. Upon the completion of cytokinesis, each daughter cell enters the G_1 phase of the cell cycle and proceeds again around the cycle.

(a)

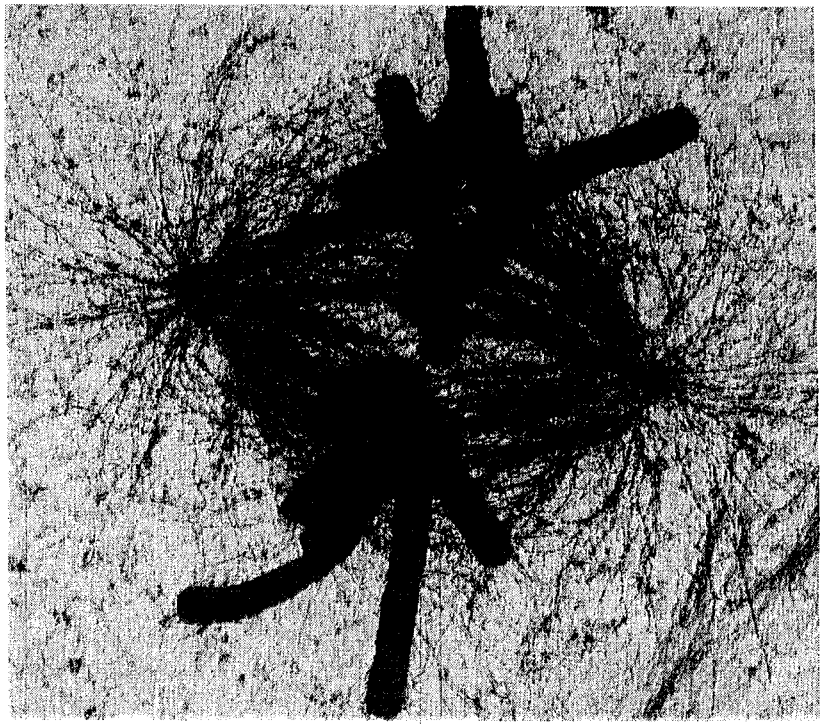

(b)

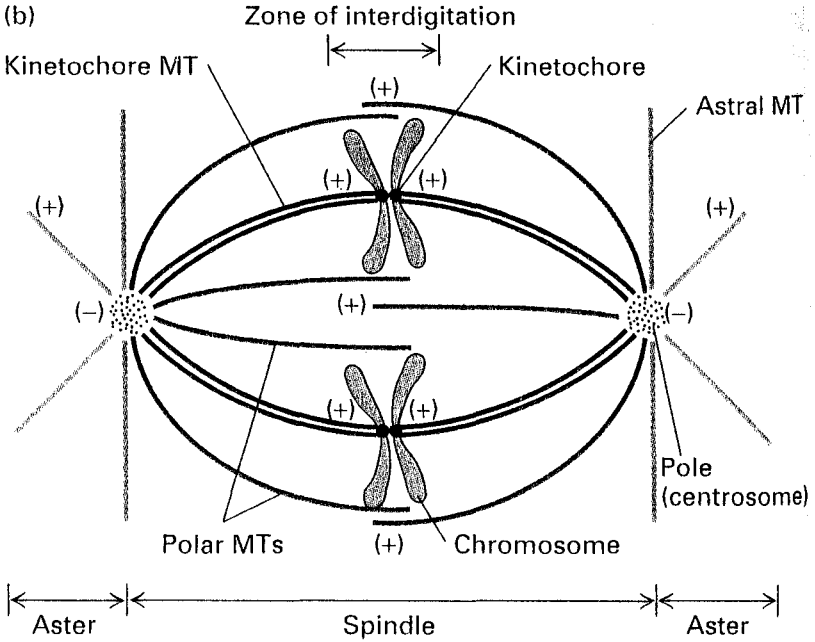

▲ FIGURE 19-36 (a) High-voltage electron micrograph of the mitotic apparatus in a metaphase mammalian cell. To visualize the spindle microtubules more clearly, biotin-tagged anti-tubulin antibodies were added to make microtubules more massive. The large cylindrical objects are chromosomes. (b) Diagram showing the three sets of microtubules (MTs) in the mitotic apparatus. Centered around the poles are astral microtubules, kinetochore microtubules, which are connected to chromosomes (blue), and polar microtubules. The (+) ends of these microtubules all point away from the centrosome at each pole. [Part (a) courtesy of J. R. McIntosh.]

2 microtubule forces:

- overlapping spindle microtubules can push spindle poles apart
- forces by astral microtubules can pull spindle poles

⇒ use laser to remove overlapping spindle microtubules ⇒ test the pulling abilities of the astral microtubules

⇒ track position of spindle poles after laser radiation

⇒ - severed poles move faster
- posterior moves faster than anterior

⇒ pulling forces + posterior stronger!

3 features:

- posterior spindle pole travels faster than anterior
- posterior spindle pole travels further
- oscillations in the proximity of cell cortex

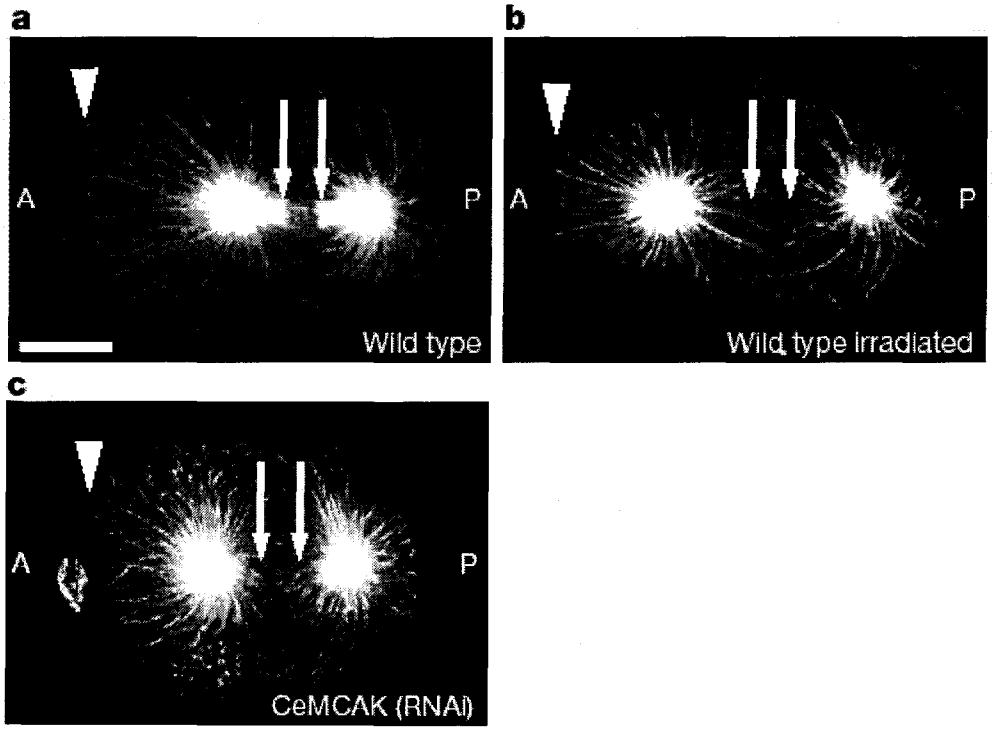

Figure 1 Spindle midzone viewed by indirect immunofluorescence with anti-tubulin antibodies. All embryos are in anaphase B. Anterior (A) is on the left and posterior (P) is on the right in this and all other figures. Scale bar, 10 μm. **a**, In wild-type embryos, both the spindle microtubules (arrows) and astral microtubules (arrowheads) are visible. **b**, **c**, Both in the wild-type irradiated and in the CeMCAK (RNAi) embryos astral microtubules are visible (arrowheads), but spindle microtubules are not (arrows).

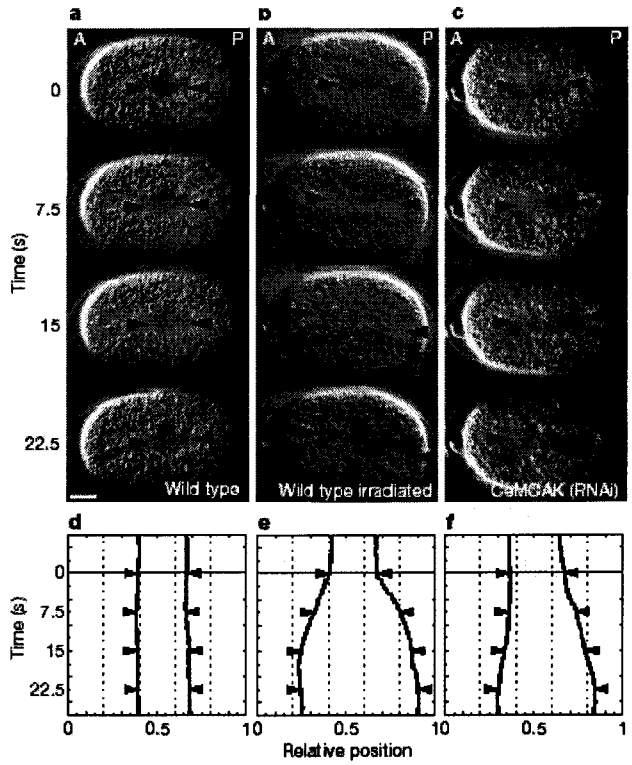

Figure 2 Pole-to-pole distance increases after spindle severing. **a–c**, Differential interference contrast (DIC) image series of *C. elegans* embryos. Spindle poles are indicated (arrowheads). Scale bar, 10 μm. **a**, Wild-type embryo. **b**, Irradiated wild-type embryo. The bar indicates where the spindle was destroyed. **c**, CeMCAK (RNAi) embryo. Spindle breakage takes place at 0 s. For both **b** and **c**, the posterior spindle pole travels further and faster than the anterior one, and a slight transverse displacement is seen in the last frame, corresponding to the beginning of transverse oscillations. Removal of ZEN-4 also results in diminished midzone microtubules without affecting anaphase B movements[29,30]. However, the timing of spindle breakage seems to be different, leading to a more subtle effect on spindle-pole velocity during anaphase (see Supplementary Information). **d–f**, Corresponding traces of relative spindle-pole position along the anterior–posterior axis, arrowheads indicate time points for which frames in **a–c** are displayed.

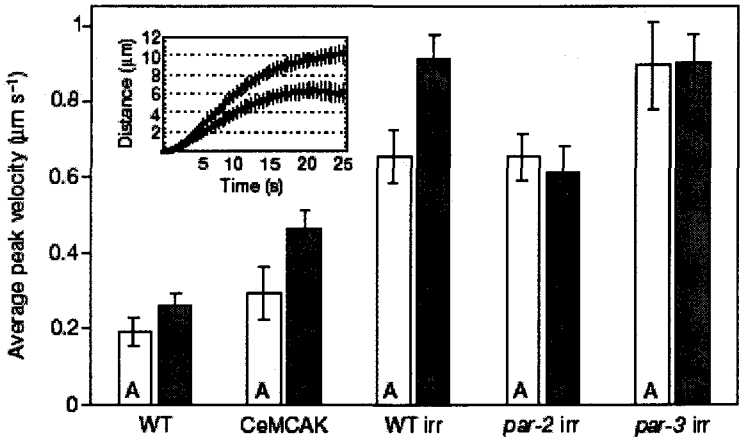

Figure 3 Average peak velocities of spindle poles increase after spindle severing. All error columns are s.e.m. with a confidence interval of 0.95. Bars show the average peak velocities of spindle poles along the anterior–posterior axis. White and black bars indicate the anterior and posterior spindle pole, respectively. Average peak velocities of spindle poles during anaphase B in wild-type (WT, $n = 20$), CeMCAK (RNAi) (CeMCAK, $n = 20$), wild-type irradiated (WT irr, $n = 34$), *par-2*(*it5*) irradiated (*par-2* irr, $n = 30$) and *par-3* (*it71*) irradiated embryos (*par-3* irr, $n = 20$) are shown. Inset, average displacement of anterior spindle pole (red) and posterior spindle pole (blue) after irradiation in wild-type embryos ($n = 34$); actual movements are in opposite directions.

numerical simulations:

show figure 4

a) posterior microtubles exert a greater pulling force
   ⇒ only achieves that posterior travels fast

b) all microtubles generate same force, at posterior microtubule density is increased
   ⇒ posterior travels faster and further but no oscillations

c) all microtubles generate the same pulling force, cortical connection is weak for posterior aster

full fills all experimental observations

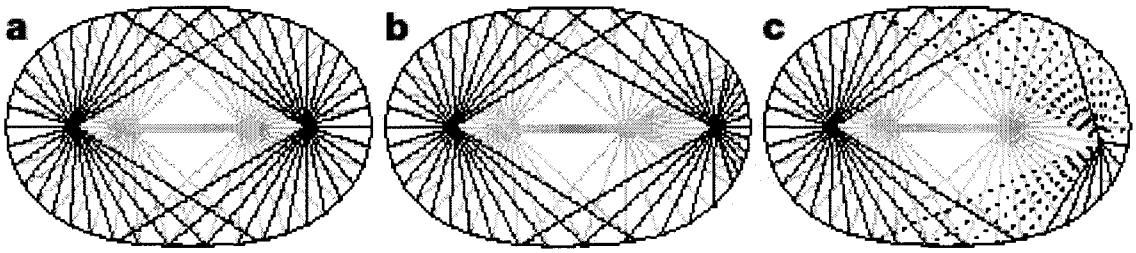

Figure 4 Numerical simulation of spindle-pole behaviour after spindle severing. The anterior aster (red) and posterior aster (blue) are shown. Grey indicates the initial state just before severing. Colours indicate the state after 22.5 s. **a**, The posterior microtubules all exert a greater pulling force than the anterior ones. **b**, All microtubules generate the same force, but the density of microtubules is increased at the very posterior end. **c**, All microtubules generate the same pulling force, but the cortical connection is weak for all microtubules of the posterior aster: they detach from the cortex instead of getting longer. Dashed lines indicate microtubules that are inactive for 12 s. Only **c** reproduces the experimental behaviour, as the posterior spindle pole travels further and faster than the anterior one, and undergoes transverse oscillations (compare with Fig. 2b and c).

c) From DNA to a Chromosome

Lit.: - L. H. Pope et al, Biophys. J., Vol 88, 2005

- ~~DNA~~ + histones ~~complexed~~ into ~~Chromatin~~

- DNA + histones form complex called chromatin
- in low salt: beads on a string
  - nucleosomes
  - linker DNA
  - DNA + histone

show figure 9-2
9-3

high salt: condensed structure
⇒ spiral of nucleosomes
six nucleosomes per turn

⇒ higher ordered structure chromosome

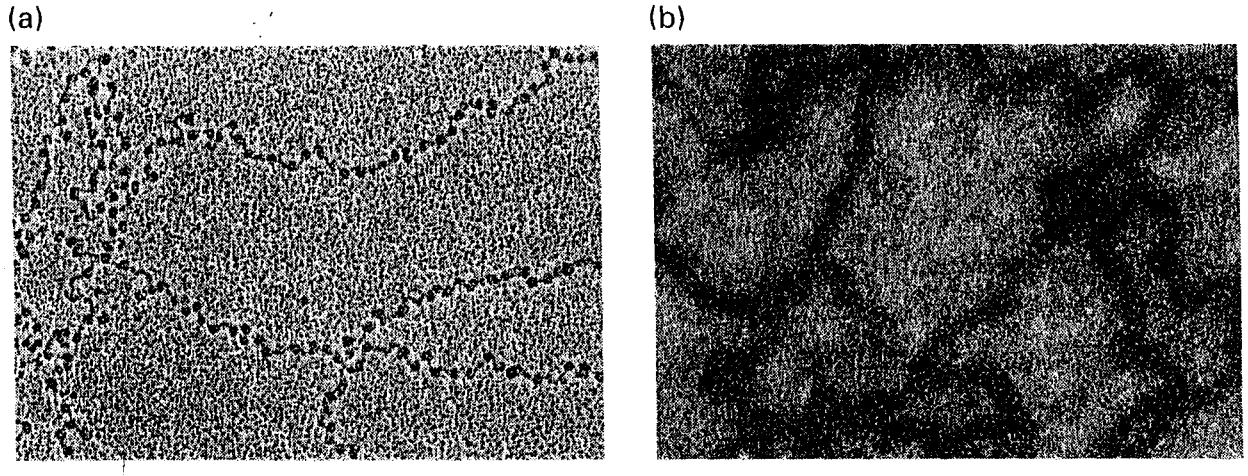

▶ **FIGURE 9-29 Electron micrographs of extracted chromatin in extended and condensed forms.** (a) Chromatin isolated in low ionic strength buffer has an extended "beads-on-a-string" appearance. The "beads" are nucleosomes (10-nm diameter) and the "string" is connecting DNA. (b) Chromatin isolated in buffer with a physiologic ionic strength (0.15 M KCl) appears as a condensed fiber 30 nm in diameter. [Part (a) courtesy of S. McKnight and O. Miller, Jr.; part (b) courtesy of B. Hamkalo and J. B. Rattner.]

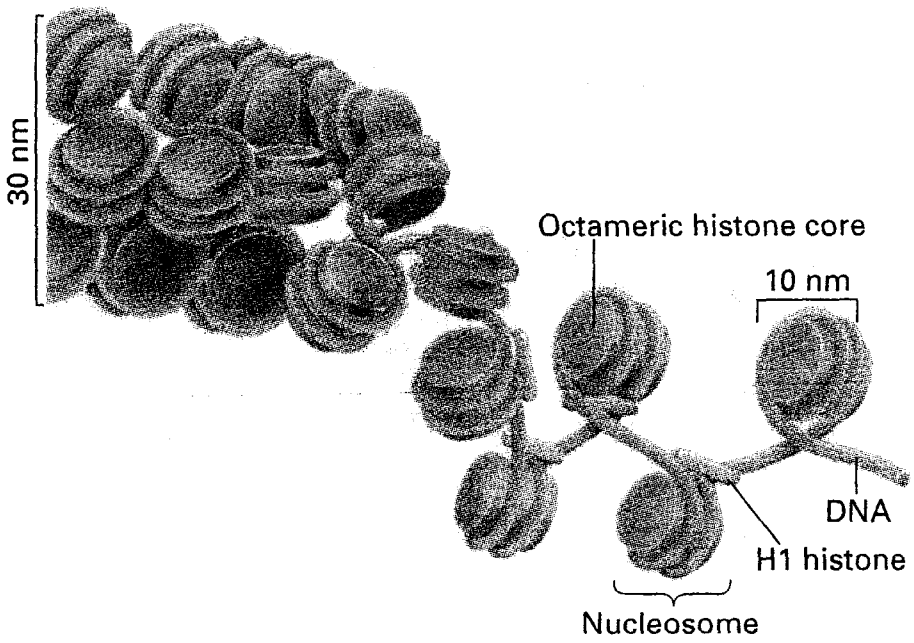

▲ FIGURE 9-31 Solenoid model of the 30-nm condensed chromatin fiber in a side view. The octameric histone core (see Figure 9-30) is shown as an orange disk. Each nucleosome associates with one H1 molecule, and the fiber coils into a solenoid structure with a diameter of 30 nm. [Adapted from M. Grunstein, 1992, *Sci. Am.* **267**:68]

ABSTRACT Eukaryotic DNA is packaged into the cell nucleus as a nucleoprotein complex, chromatin. Despite this condensed state, access to the DNA sequence must occur during gene expression and other essential genetic events. Here we employ optical tweezers stretching of reconstituted chromatin fibers to investigate the release of DNA from its protein-bound structure. Analysis of fiber length increase per unbinding event revealed discrete values of ~30 and ~60 nm. Furthermore, a loading rate analysis of the disruption forces revealed three individual energy barriers. The heights of these barriers were found to be ~20 k_BT, ~25 k_BT, and ~28 k_BT. For subsequent stretches of the fiber it was found that events corresponding to the ~28 k_BT energy barrier were significantly reduced. No correlation between energy barrier crossed and DNA length release was found. These studies clearly demonstrate that optical tweezers stretching of chromatin provides insight into the energetic penalties imposed by chromatin structure. Furthermore these studies reveal possible pathways via which chromatin may be disrupted during genetic code access.

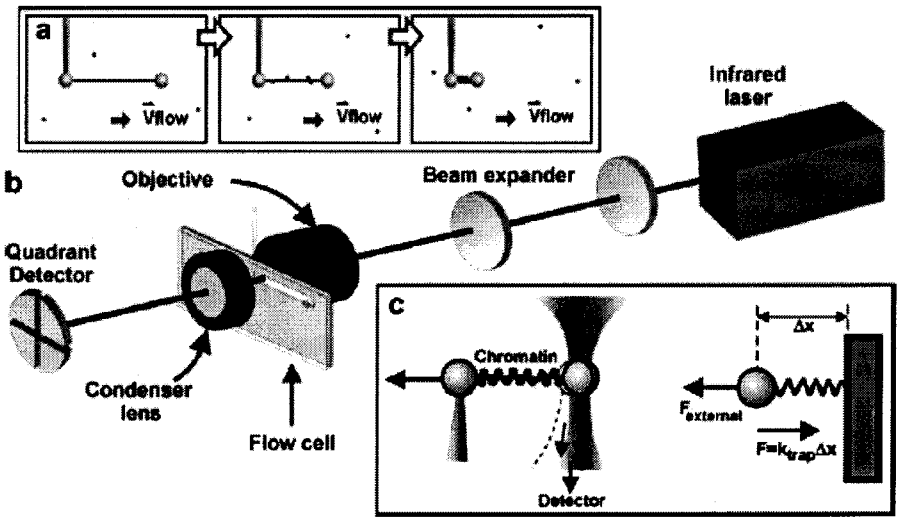

FIGURE 1 An illustration of the experimental setup. (*a*) After the capture of a single DNA molecule between two beads the *Xenopus* extract is added to the flow chamber. A very slow flow rate of <50 μm/s is used that corresponds to the application of low forces <1 pN on the DNA molecule. The molecule condenses from 16.4 to 2 μm in length. (*b*) The experimental setup comprises of a 1064-nm infrared laser, which is expanded to fill the back aperture of a water immersion objective lens. The objective focuses the laser to a spot in the center of the flow channel, hence establishing the optical trap. A piezo-driven flow cell with an integrated glass micropipette is employed to allow movement of the nontrapped bead. A CCD camera is used to track the distance between the two beads (not shown). A quadrant detector monitors deflections of the transmitted laser light from the trapped bead. (*c*) As the chromatin fiber is stretched the trapped bead is displaced by Δx from its zero-force position. This deflection is directly proportional to the tension within the molecule under investigation; hence the trap behaves as a simple Hookean spring for small bead displacements (<0.5 μm). It should be noted that the trap stiffness k_{trap} is chosen to ensure measurements are within the linear range of the detector ($k_{trap} \approx 100$ pN/μm).

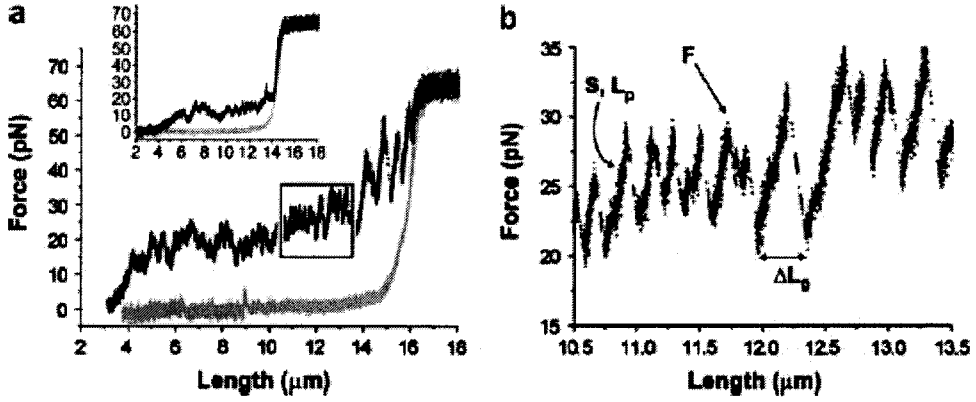

FIGURE 2 (*a*) The first and second (*inset*) stretch of a reconstituted chromatin fiber. The force-extension data were collected from a single DNA molecule incubated with *Xenopus* egg extract. The stretch curve is shown in black and the relax curve is shown in gray. (*b*) An enlargement of a small portion (*box* in panel *a*) of the chromatin stretch curve reveals discrete unbinding events, observed here as steps in the data. From each individual step information can be extracted about the mechanical properties of the fiber, such as persistence length (L_p) and stretch modulus (S). A study of rupture force (F) versus loading rate can be used to study the energetics and kinetics of interactions that are disrupted during the chromatin fiber stretch. The change in length for a single force value is essentially the change in fiber contour length ΔL_0, assuming that the mechanical properties of the fiber remain virtually unchanged after a single unbinding event.